Int. J. Electrochem. Sci., 3 **(2008)** 291 - 301

International Journal of
ELECTROCHEMICAL
SCIENCE
www.electrochemsci.org

Improved Voltammograms of Hydrocaffeic Acid on the Single-Walled Carbon Nanotube/Graphite-Film Surfaces

Abdolmajid Bayandori Moghaddam [1,*], *Mahmood Kazemzad* [2], *Mohammad Reza Nabid* [3], *Habibeh Haddad Dabaghi* [4]

[1] Department of Medical Chemistry, School of Pharmacy, Shahid Beheshti University of Medical Sciences, P. O. Box: 14155-6153, Tehran, Iran
[2] Department of Energy, Materials and Energy Research Center, P.O. Box 14155-4777, Tehran, Iran
[3] Department of Chemistry, Faculty of Science, Shahid Beheshti University, Tehran 1983963113, Iran
[4] Department of Science, Karaj Branch, Islamic Azad University, Karaj, Iran
[*]E-mail: bayandori@gmail.com

Received: 15 November 2007 / *Accepted:* 6 January 2008 / *Online published:* 20 January 2008

The performance of a single-walled carbon nanotube (SWCNT)/graphite-film electrode, prepared by mixing SWCNTs and graphite powder in equal weight fractions with a small amount of paraffin, was investigated. The electrode shows excellent electrochemical behavior for the redox of hydrocaffeic acid (HCA), an important biological molecule. It gives a significant decrease in overvoltage for HCA oxidation as well as a dramatic improvement in reversibility of the HCA redox behavior in comparison with the graphite-film and glassy carbon electrodes.

Keywords: single-walled carbon nanotube; cyclic voltammetry; hydrocaffeic acid; nanoscience; nanotechnology

1. INTRODUCTION

The rapid progress in nanotechnology and nanoscience introduce a scientific momentum that involves fundamental understanding of the properties of nanostructures [1], synthesis and plans in nanoscale. Since the days of Michael Faraday, different carbon structures have been studied as electrode material. Presently, electrodes made from various carbon materials (partially graphitized glassy carbon, activated carbon and graphite fibers) are widely used in important electrochemical applications [2-5]. The work reported by Adams in 1958 [6], carbon composite electrodes have received enormous attention. Among them, composites made of graphite powder and mineral oil are the most widely known [7]. In 1991, Iijima discovered microtubules of graphitic carbon with outer diameters of 4-30 nm and a length of up to 1 μm, naming these tubes multi-walled carbon nanotubes

(MWCNTs) [8]. In addition, a report of carbon fibers down to 4 nm in diameter, found on a carbon arc electrode, was published by Wiles and co-workers [9,10]. Single-walled carbon nanotubes (SWCNTs), which are seamless cylinders each made of a single graphene sheet, were first reported in 1993 [11,12]. The closed topological and tubular structure of carbon nanotubes make them unique among different carbon forms and provide pathways for chemical studies. A number of investigations carried out to find applications of carbon nanotubes in modified electrode could impart strong electrocatalytic activity to some important biomolecules [13-17].

Phenolic compounds are important constituents of apple derivatives because they greatly contribute to their sensory properties and other attributes. In particular, polyphenolic compounds have antioxidant activity, free-radical scavenging capacity, coronary heart disease prevention and anticarcinogenic properties [18-20]. Furthermore, phenolics are associated with bitterness, astringency, color stability and some of them have been used for detecting adulterations in apple products and could be inhibitors for microbiological growth-avoiding process spoilages [21,22]. In addition, caffeic acid esters, such as caffeic acid phenethyl (CAPE) and benzyl esters, display selective antiproliferative activity against some types of cancer cells [23]. For these reasons, knowledge of the redox properties of hydrocaffeic acid (HCA) is important for a better understanding of their behavior in biological environments. Moreover, the electrochemical method is rapid and inexpensive for the study of this important category of molecules [2] and others [24-27]. We report here, the HCA electrochemical behavior at a SWCNT/graphite-film electrode by cyclic voltammetry (CV).

2. EXPERIMENTAL PART

2.1. Materials

Hydrocaffeic acid (Aldrich), graphite powder, acids and the used salts (Merck) for preparation of the buffer solutions were reagent grade materials and used without any further purification. Single-walled carbon nanotubes (SWCNTs) purchased from Research Institute of Petroleum Industry (Iran). All solutions were prepared with deionized water.

2.2. Apparatus

All electrochemical experiments were performed by the Autolab potentiostat PGSTAT 30 (Eco Chemie, Netherlands), equipped with the GPES 4.9 software, including a three-electrode cell; a glassy-carbon (GC), graphite and SWCNT/graphite-film acted as working electrodes, a platinum wire as counter electrode and Ag|AgCl|KCl (sat.) as reference electrode. All potentials are reported with respect to this reference. All experiments were carried out at 25 ± 1 °C.

Furthermore, the microscopic studies related to transmission electron microscopy (TEM) were performed using a Phillips transmission electron microscope, the scanning electron microscopy (SEM) were recorded using a ZEISS DSM 960, while the atomic force microscopy (AFM) were performed with the help of a DME, controller: Dual Scope C-21, and scanner: DS 95-50.

Gaussian 98, Revision A. 6, program has been used for the quantum mechanic calculations. The B3LYP/6-31G* method is employed for gas-phase molecular geometry and HF/6-31G* method is used for obtained atomic charges (ESP fit) [28]. Note that the limitation of this approach is that the polarization effect associated with condensed phase environment is not explicitly included, although tendency for the HF/6-31G* QM (Quantum Mechanics) level of theory to overestimate dipole moments has been suggested to account for this deficiency [29].

2.3. Preparation of the SWCNT/graphite-film electrode

For electrochemical studies, the SWCNT/graphite-film electrodes were prepared from a mixture of SWCNTs and graphite powder in the ratio of 1:1 (w/w). Regarding the casting procedure, a small amount of melted paraffin (~ 20 % by weight) was added to SWCNT/graphite powder mixture. A portion of composite mixture was packed into the end of a polyamide tube. The electrical contact was made by forcing a glassy carbon rod (r = 1.5 mm) down into the tube and into back of the composite and, then, a thin film on the surface of glassy carbon electrode. This strategy increased the compactness and stability of composite on the surface of glassy carbon electrode. Here, it should be mentioned that only a very small amount of melted paraffin had to be used for the attachment of composite, because in this way a hard composite creation was achieved, illustrating excellent electrochemical properties. In addition, the employment of a greater melted paraffin amount raised the peak potentials. Pure SWCNT or graphite-film electrodes were also made using the separate materials, dispersed in a small quantity of melted paraffin, in the same way as for composite electrodes described above. The GC rod was carefully polished with alumina (1, 0.3 and 0.05 μm, respectively) by a polishing cloth. The electrode was placed in ethanol and deionized water sonicated to remove the adsorbed particles.

3. RESULTS AND DISCUSSION

3.1. SEM, TEM and AFM characterization

Fig. 1(a) illustrates the scanning electron microscopic (SEM) images and Fig. 1(b) depicts the transmission electron microscopic (TEM) image of SWCNTs structure.

Fig. 2 (a and b) presents the AFM images of a SWVNT. Additionally, Fig. 2 (c and d) depicts image profiles of the SWCNT. This profiles display the SWCNT diameter in top, middle, and bottom for selected points in AFM image with the values of 18.0, 42.3, and 82.3 nm (Fig. 2c) and 5.83, 17.7, and 35.2 nm (Fig. 2d).

3.2. Electrochemical behavior of HCA at the SWCNT/graphite-film electrode

Fig. 3 depicts typical cyclic voltammograms (CVs) obtained from GC electrode (a), graphite-film electrode (b) and SWCNT/graphite-film electrode (c) after the addition of 0.06 mM hydrocaffeic acid (HCA). The presence of well-defined reversible anodic and cathodic peaks indicated improved

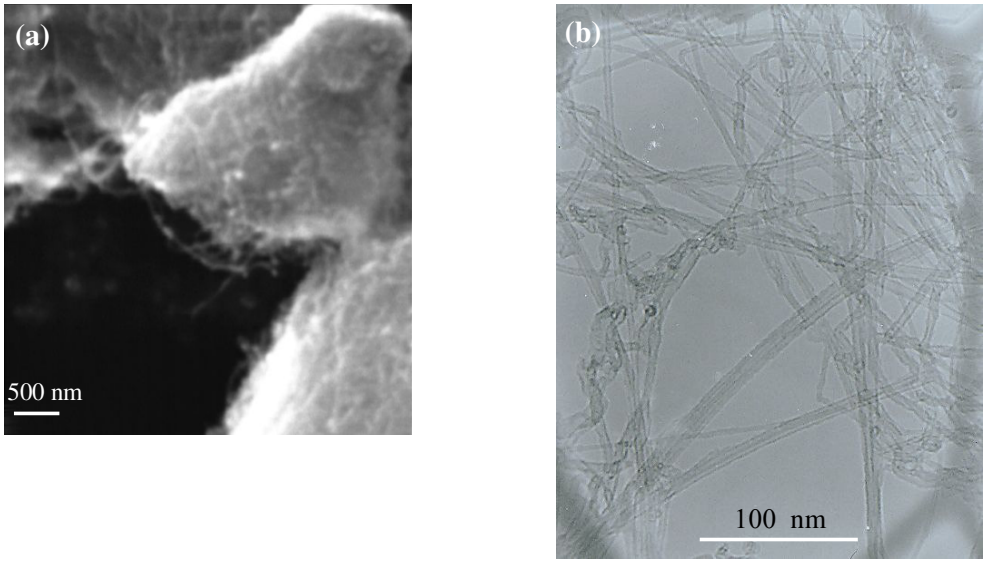

Figure 1. (a) SEM images and (b) TEM image of the SWCNTs.

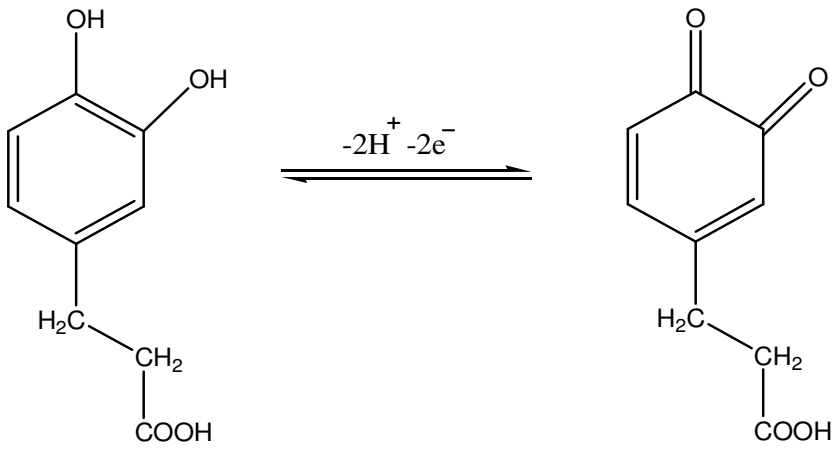

Scheme 1. Redox mechanism of HCA.

electrochemical reactivity for HCA oxidation-reduction reaction in accordance to Scheme 1 [2, 24, 25] on the SWCNT/graphite-film electrode. The CVs show a characteristic anodic peak at E_{pa} = 0.305 V for a GC electrode, at E_{pa} = 0.299 V for a graphite-film electrode and at E_{pa} = 0.259 V *vs.* Ag | AgCl | KCl, sat. for a SWCNT/graphite-film electrode and the complementary cathodic peak at E_{pc} = 0.155 V for a GC, at 0.146 V for a graphite and at 0.207 V for SWCNT/graphite-film electrode. The difference between E_{pa} and E_{pc} (ΔEp) decreased from 0.150 V for GC, 0.153 V for graphite to 0.052 V in SWCNT/graphite-film electrode. Thus, reversibility of HCA was significantly improved. The peak current also increased greatly for SWCNT/graphite-film electrode in contrast to graphite-based electrode. The reason for the better performance of SWCNT/graphite-film electrode may be due to the nanometer dimensions of SWCNTs, electronic structure and the present of large numbers of

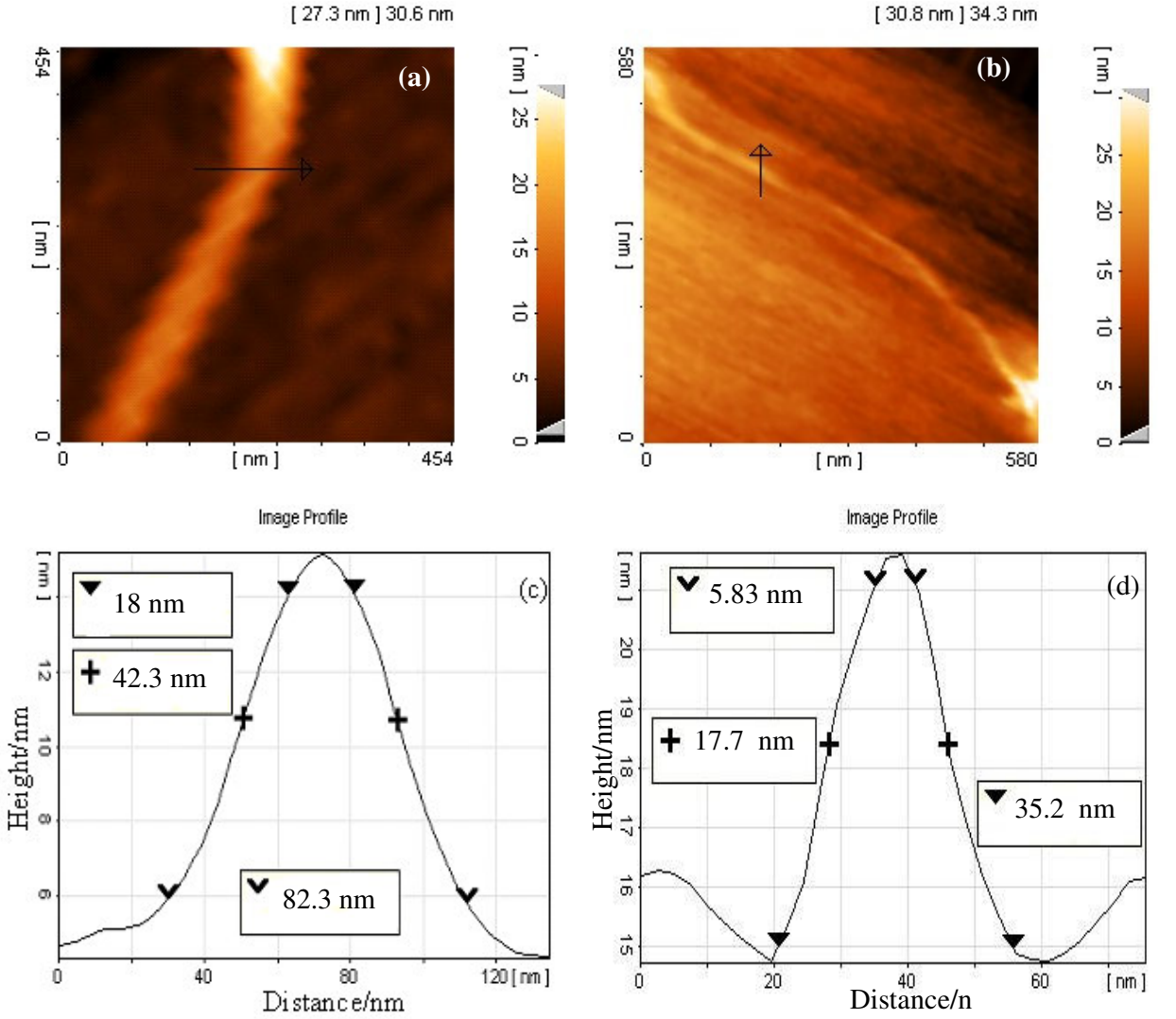

Figure 2. (a) and (b) AFM images for SWCNTs, (c) and (d) the obtained image profiles for (a) and (b), respectively.

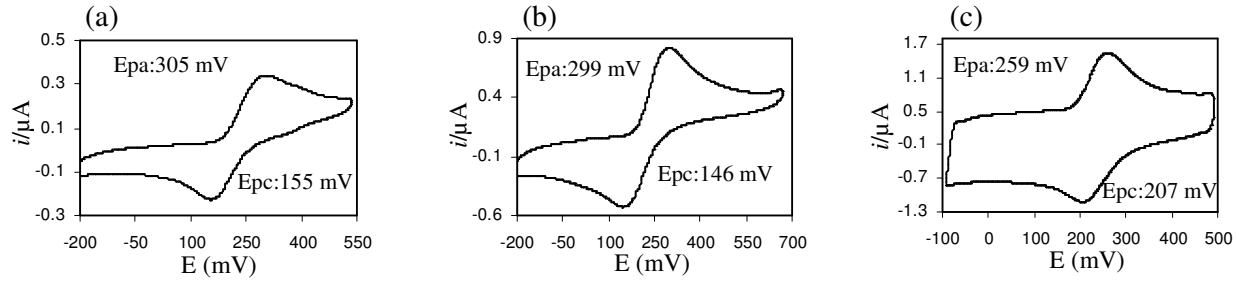

Figure 3. Comparative cyclic voltammograms of 0.06 mM HCA on the surface of (a) GC electrode (b) graphite-film electrode and (c) SWCNT/graphite-film electrode in PBS (pH = 6.0, c = 0.15 M). Scan rate: 0.025 V.s^{-1}.

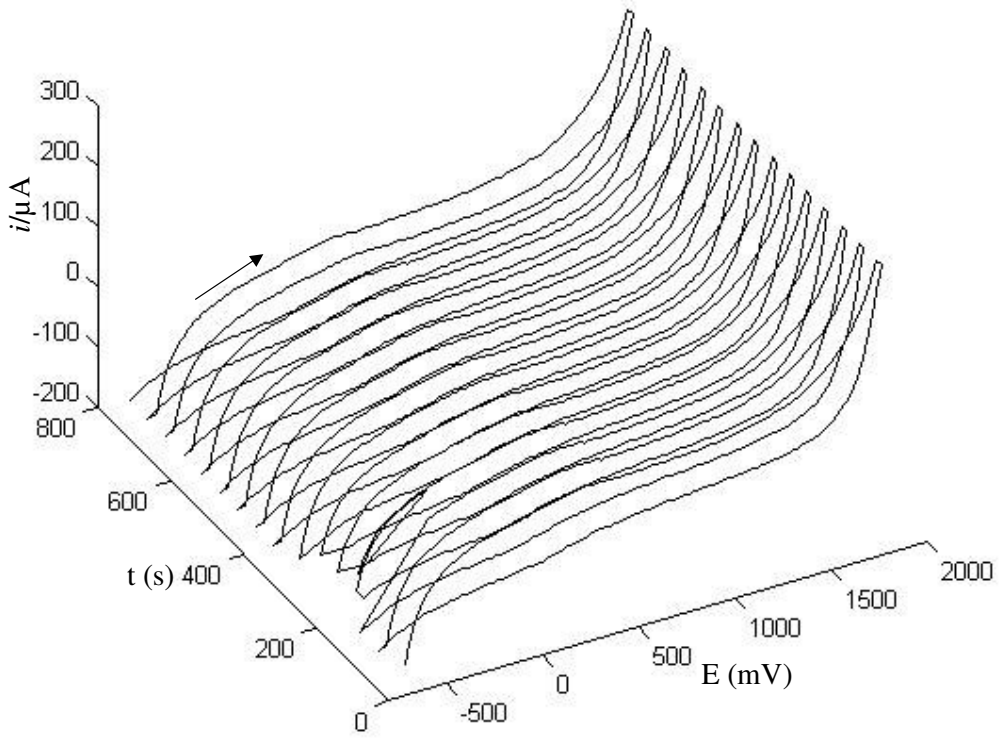

Figure 4. Electrochemical behavior of the SWCNT/graphite-film electrode during the continuous cyclic voltammograms, scan rate; 0.1 $V.s^{-1}$.

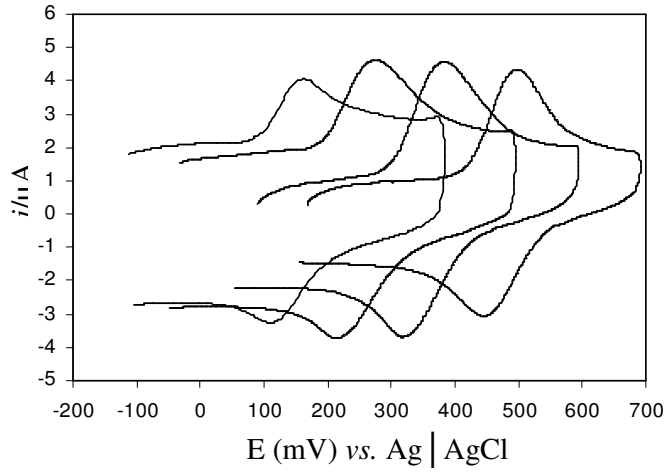

Figure 5. Cyclic voltammograms of 0.06 mM HCA on the surface of SWCNT/graphite-film electrode in various pH values (c = 0.15 M) from positive potentials to negative potentials, pH = 2, 4, 6 and 8. Scan rate: 0.1 $V.s^{-1}$.

topological defects (e.g., bond rotational defects or pairs of 5-7 rings; defects which would not create any visible change in the overall topology or curvature) has been suggested [14]. Hence, the surface of

nanotubes could be inherently more reactive compared to their graphite counterparts [30]. Depending on their atomic structure, CNTs behave electrically as a metal or as a semiconductor [31]. The subtle electronic properties suggest that CNTs have the ability to promote electron-transfer reactions, when used as an electrode in chemical reactions [32]. In the meantime, SWCNTs augment the effective area

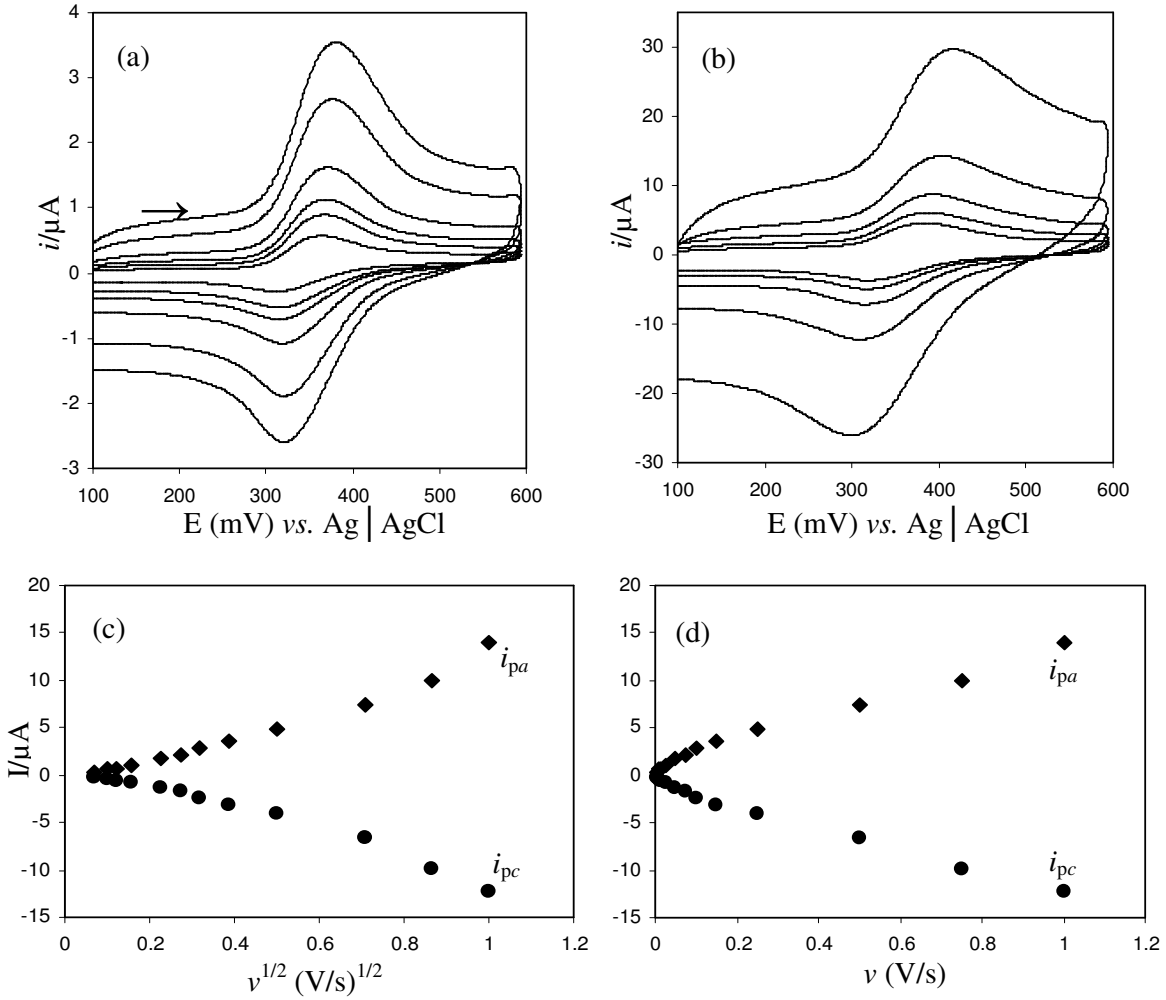

Figure 6. (a and b) Cyclic voltammograms of HCA in PBS (pH = 4.0) at various sweep rates. From outer to inner; 1, 0.5, 0.25, 0.15, 0.1, 0.075, 0.05, 0.025, 0.015, 0.01 and 0.005 V.s^{-1}, other conditions as in Fig. 5. The plots of anodic and cathodic peak currents *vs.* (c) square root of scan rate and (d) scan rate.

of electrode. The modified electrode has no electrochemical activity in used solutions, but the background current becomes larger, which is attributed to the fact that SWCNTs can increase the surface activity noticeably (Fig. 4). Further explore on the effect of SWCNTs on electrochemical process, we studied pH effect on the response of modified electrode by cyclic voltammetry. Fig. 5 demonstrates the CVs of 0.06 mM HCA in different buffer solutions (c = 0.15 M) with various pH values, with increasing the pH of solution HCA formal potential $E^{\circ'}$ (taken as the average of reduction and oxidation peak potentials in the cyclic voltammogram) shifted negatively, from 0.472 V (pH = 2.0)

to 0.351 V (pH = 3.0), 0.243 V (pH = 6.0) and 0.135 V (pH = 8.0). To further investigate the characteristics of HCA at SWCNT/graphite-film electrode surface, influence of scan rate on the oxidation of HCA was studied by cyclic voltammetry (Fig. 6a-d). With increasing scan rate, the peak current grows. There is a good linear relationship between the peak current and scan rate (v) in the range of 0.005-1.0 $V.s^{-1}$ (Fig. 6d). This means that the electrode process is controlled by adsorption. On the other hand, with the increase of scan rates, the oxidation peak shifts to more positive potentials, while the reduction peak shifts to more negative potentials, indicating that the electron-transfer rate is not very fast and the electrochemical reaction gradually becomes less reversible.

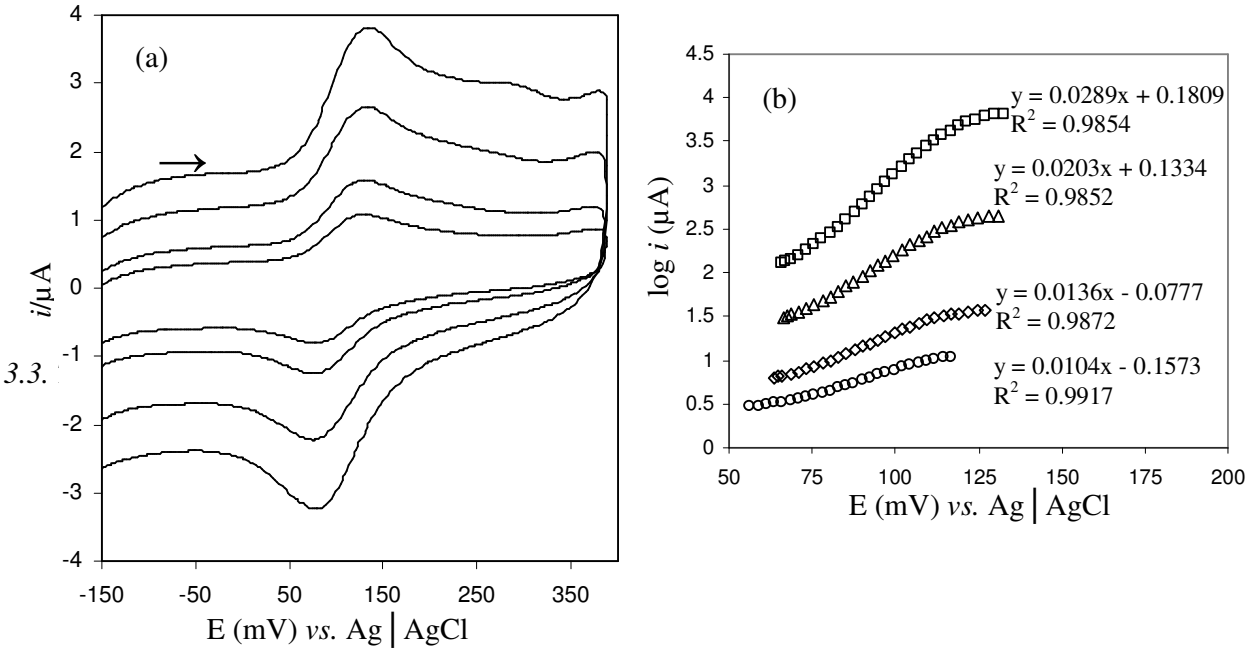

Figure 7. (a) Cyclic voltammograms of HCA in carbonate buffer (pH = 9.0) at various sweep rates. (b) The Tafel plots for the rinsing part of the oxidation peaks of CVs, which related to the scan rates (from bottom to top): 0.015, 0.025, 0.050 and 0.075 $V.s^{-1}$, other conditions as in Fig. 5.

Fig. 7 depicts the CVs of HCA at pH = 9.0 in various scan rates. In the evaluating kinetic parameters, Tafel plots were obtained from the increasing part of anodic branch between 15 and 75 $mV.s^{-1}$ at a SWCNT/graphite-film electrode (Fig. 7b). Because the Tafel plot for anodic branch has the slope of (1-α) $nF/2.303RT$, it is affected by the electron transfer kinetics between HCA and the electrode surface, assuming HCA deprotonation is a fast step. In this condition, the number of transferred electrons can estimated from slop of the Tafel plot.

The influence of scan rate on the HCA oxidation at graphite-film electrode was studied by cyclic voltammetry. Fig. 8 depicts anodic and cathodic peak currents of HCA at the graphite-film electrode in pH = 7.0 at various scan rates. According to Fig. 8a, the redox peak currents of HCA

increased linearly with the square root of scan rate. This means that HCA electrochemical behavior at the graphite-film electrode was a diffusion-controlled process.

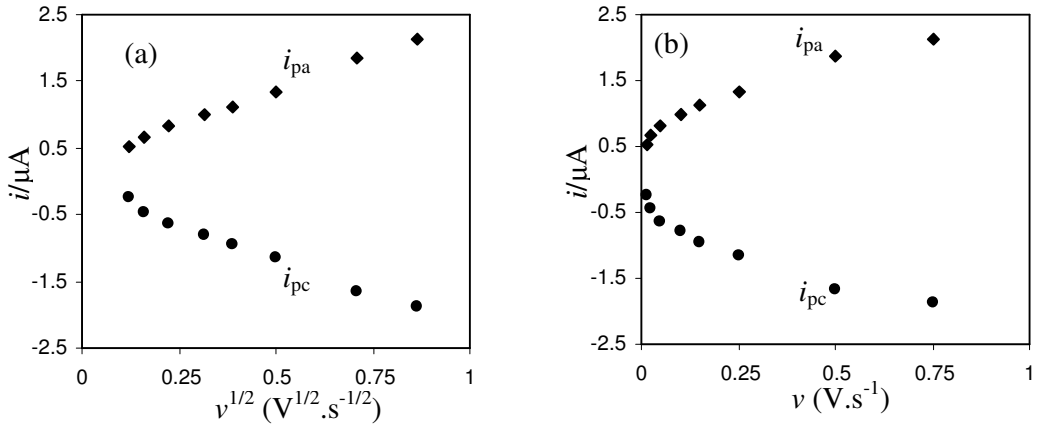

Figure 8. The relationship between the peak currents (i_{pa}, i_{pc}) *vs.* the square root of the sweep rates (a) and sweep rates (b) for 0.06 mM HCA at the graphite-film electrode in PBS (pH = 7.0) at 0.015, 0.025, 0.05, 0.10, 0.15, 0.25, 0.50 and 0.75 V.s^{-1}.

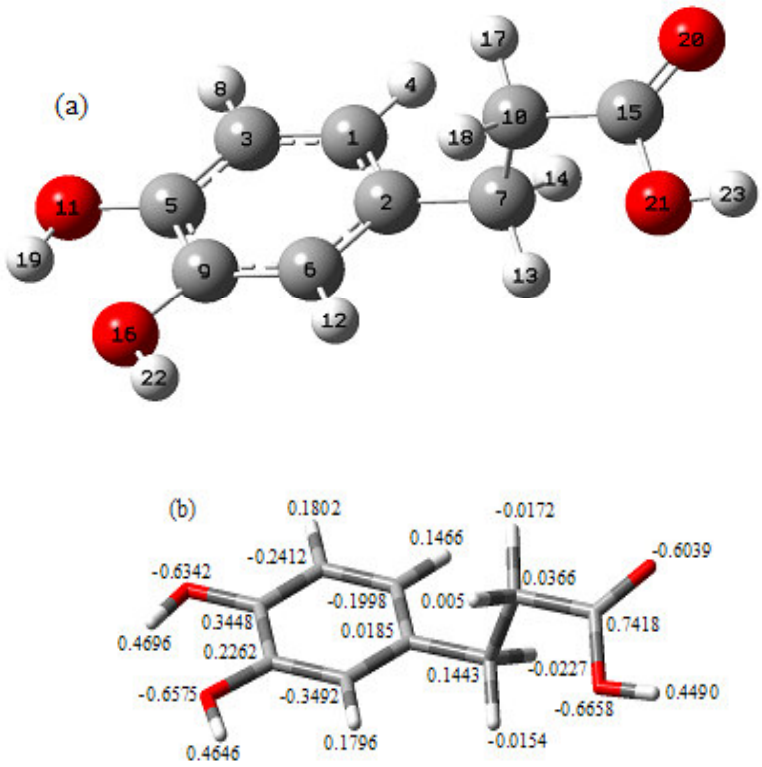

Figure 9. (a) Optimized geometry (B3LYP/6-31G*) of HCA, and (b) atomic charges of HCA

On the one hand, electrode process was controlled by adsorption on the surface of SWCNT/graphite-film electrode (Fig. 6) and it was controlled by diffusion on the surface of graphite-

film electrode (Fig. 8). On the other hand, during the HCA electro-oxidation, positive potentials were applied to the electrode. Therefore, HCA atoms with the more negative charges could be the adsorbed sites of HCA on the SWCNTs surfaces. For this reason, calculation of HCA atomic charges might be very useful. The HCA atomic charges are presented in Fig. 9. According to HCA atomic charge, the higher negative charges are related to the oxygen atoms and the highest negative charge among the oxygen atoms is attributed to the oxygen atom of the hydroxyl group in carboxylic acid group. In detail, the oxygen atom of hydroxyl in carboxylic acid group presents the highest negative charge (-0.6658), in contrast to the other oxygen atoms, which exhibits negative charge values of -0.6575, -0.6342 and -0.6039. Therefore, the carbon atom in the carboxylic acid group displays the highest positive charge (0.7418). The carbon atoms in aromatic ring are negatively charged. Nevertheless, in the aromatic ring with electron-withdrawing groups, the carbon atoms, which are connected to these kinds of groups, are positively charged.

4. CONCLUSIONS

The properties of SWCNT/graphite-film electrode have been demonstrated. SWCNT/graphite-film electrode offers a diametric improvement in the electrochemical behavior of hydrocaffeic acid (HCA). A pair of well-defined redox waves obtained. The SWCNT/graphite-film electrode showed promising promotion of HCA electrochemical reaction. The attractive properties of this new composite material open a new entrance for new electrodes in the field of electrochemical applications.

In one hand, electron transfer plays a pivotal role in biological functions essential to life and the other hand, novel electrode surfaces that act as efficient interfaces for transferring electrons significantly broaden the repertoire of reactions that are electrochemically accessible. Therefore, nanotechnology can extremely influence the development rate of these scientific fields. Escalating attention in electrochemistry of biologically important molecules is driven by remarkable progress in designing efficient interfaces for transferring electrons between electrode surfaces and biologically important molecules.

References

1. H. J. Wang, C. M. Zhou, F. Peng, H. Yu, *Int. J. Electrochem. Sci.* 2 (2007) 508.
2. A. Bayandori Moghaddam, F. Kobarfard, A. R. Fakhari, D. Nematollahi, S. S. Hosseiny Davarani, *Electrochim. Acta* 51 (2005) 739.
3. A. Bayandori Moghaddam, F. Kobarfard, S. S. Hosseiny Davarani, D. Nematollahi, M. Shamsipur, A. R. Fakhari, *J. Electroanal. Chem.* 586 (2006) 161.
4. S. Ranganathan, T. Kuo, R. L. McCreery, *Anal. Chem.,* 71 (1999) 3574.
5. J. H. Kim, K.-W. Nam, S. B. Ma, K. B. Kim, *Carbon* 44 (2006) 1963.
6. R. N. Adams, *Anal. Chem.* 30 (1958) 1576.
7. K. Kalcher, J. M. Kauffmann, J. Wang, I. Svacara, K. Vytras, C. Neuhold, *Electroanalysis* 7 (1995) 5.
8. S. Iijima, *Nature* 354 (1991) 56.
9. P. G. Wiles, J. Abrahamson, *Carbon* 16 (1978) 341.
10. J. Abrahamson, P. G. Wiles, B. L. Rhoades, *Carbon* 37 (1999) 1873.

11. S. Iijima, T. Ichihashi, *Nature* 36 (1993) 603.
12. D. S. Bethune, C. H. Kiang, M. D. Vries, G. Gorman, V. Savoy, J. Vazquez, *Nature* 363 (1993) 605.
13. P. Xiao, Q. Zhou, F. Xiao, F. Zhao, B. Zeng, *Int. J. Electrochem. Sci.* 1 (2006) 228.
14. A. Salimi, A. Noorbakhash, F. S. Karonian, *Int. J. Electrochem. Sci.* 1 (2006) 435.
15. P. Xiao, W. Wu, J.Yu, F. Zhao, *Int. J. Electrochem. Sci.* 2 (2006) 149.
16. J. Wang, M. Musameh, Y. Lin, *J. Am. Chem. Soc.* 125 (2003) 2408.
17. K.-H. Xue, F.-F. Tao, S.-Y. Yin, W. Shen, W. Xu *Chem. Phys. Lett.* 391 (2004) 243.
18. M. S. Dupont, R. N. Bennet, F. A. Mellon, G. Williamson, *J. Nutr.* 132 (2002) 172.
19. H, Lentowics, S. Gorinstein, A. Lojej, M. Leontowicz, M. Ciz, R. Soliva-Fortuny, *J. Nutr. Biochem.* 13 (2002) 603.
20. F. Chinnici, A. Bendini, A. Gaiani, C. Riponi, *J. Agric. Food. Chem.* 52 (2004) 4684.
21. M. M. Cowan, *Clin. Microbiol. Rev.* 12 (1999) 564.
22. G. A. Spanos, R. E. Wrolstad, *J. Agric. Food Chem.* 40 (1992) 1478.
23. T. Nagaoka, A. H. Banskota, Y. Tezuka, I. Saiki, S. Kadota, *Bioorg. Med. Chem.* 10 (2002) 3351.
24. W. Sun, M. Yang, K. Jiao, *Int. J. Electrochem. Sci.* 2 (2007) 93.
25. G. G. Wildgoose, A. T. Masheter, A. Crossley, J. H. Jones, R. G. Compton, *Int. J. Electrochem. Sci.* 2 (2007) 809.
26. J. Zhao, X. Zheng, W. Xing, J. Huang, G. Li *Int. J. Mol. Sci.* 8 (2007) 42.
27. R. Lao, L. Wang, Y. Wan, J. Zhang, S. Song, Z. Zhang, C. Fan, L. He, *Int. J. Mol. Sci.* 8 (2007) 136.
28. GAUSSIAN 98, Revision A.6, Gaussian, Inc. Pittsburgh PA, 1998.
29. O. M. Becker, A. D. McKerell Jr., B. Roux, M. Watanabe, Computational Biochemistry and Biophysics, Marcel Dekker Inc., New York (2001) 21.
30. D. Tekleab, R. Czerw, D. L. Carroll, P. M. Ajayan, *Appl. Phys. Lett.* 76 (2000) 3594.
31. J. M. Nugent, K. S. V. Santhanam, A. Rubio, P. M. Ajayan, *Nano Lett.* 1 (2001) 87.
32. R. S. Nicholson, I. Shain, *Anal. Chem.* 36 (1964) 706.